Megawatt Power Generation of the Dual-Frequency Gyrotron for TCV at 84 and 126 GHz, in Long Pulses

J.-P. Hogge[1, a)], S. Alberti[1], K. A. Avramidis[2], A. Bruschi[3], W. Bin[3], F. Cau[4], F. Cismondi[5], J. Dubray[1], D. Fasel[1], G. Gantenbein[2], S. Garavaglia[3], J. Genoud[1], T. P. Goodman[1], S. Illy[2], J. Jin[2], F. Legrand[6], R. Marchesin[3], B. Marlétaz[1], J. Masur[1], A. Moro[3], C. Moura[1], I. Gr. Pagonakis[2], E. Périal[6], L. Savoldi[7], T. Scherer[8], U. Siravo[1], M. Thumm[2], M. Toussaint[1] and M.-Q. Tran[1]

[1]*EPFL-Swiss Plasma Center (SPC), CH-1015 Lausanne, Switzerland.*
[2]*IHM, Karlsruhe Institute of Technology, 76131 Karlsruhe, Germany.*
[3]*Istituto di Scienza e Tecnologia dei Plasmi (ISTP), Consiglio Nazionale delle Ricerche, Milan, Italy.*
[4]*Fusion for Energy, 08019 Barcelona, Spain.*
[5]*Euro-Fusion, Boltzmannstrasse 2, 85748 Garching, Germany.*
[6]*Microwave Imaging Solution, THALES, Vélizy-Villacoublay, F-78141, France.*
[7]*NEMO Group, Dipartimento Energia, Politecnico Di Torino (POLITO), 10129, Torino, Italy.*
[8]*Institut für Angewandte Materialien, KIT, Kaiserstr. 12, D-76131 Karlsruhe, Germany.*

[a)]Corresponding author: jean-philippe.hogge@epfl.ch

Abstract. In the frame of the TCV Tokamak upgrade, two 84/126 GHz/2 s dual frequency gyrotrons designed by SPC and KIT and manufactured by THALES will be added to the existing EC-System. The first unit has been delivered to EPFL-SPC and tested. In the commissioning configuration, a matching optics unit (MOU) is connected to the gyrotron window. The RF is then coupled to the HE_{11} mode of a 63.5mm corrugated waveguide and dissipated in a load procured by CNR after 4m of waveguide and 2 miter bends. Owing to the flexible triode gun design giving the possibility to adjust the pitch angle parameter, the specifications were met at both frequencies. At 84 GHz ($TE_{17,5}$ mode), a power of 0.930 MW was measured in the calorimeter, with a pulse duration of 1.1 s. At the high frequency (126 GHz, $TE_{26,7}$ mode), a power of 1.04 MW was reached for a pulse length of 1.2 s. Accounting for the load reflection and the ohmic losses in the various subcomponents of the transmission line and the tube, it is estimated that the output power at the gyrotron window is in excess of 1 MW at both frequencies, with an electronic efficiency of 32% and 34% at 84 GHz and 126 GHz respectively. The gyrotron behavior is remarkably robust and reproducible, and the pulse length is limited by external systems that will be improved shortly.

INTRODUCTION AND TUBE DESIGN

The TCV tokamak is undergoing an upgrade [1] which includes an increase of the EC power by adding two gyrotron units capable to deliver a total of 2 MW either at the second harmonic (X2, 84 GHz) in low field side injection or at the third harmonic (X3, 126 GHz) in top-launch configuration [2].

The tube design is largely based on the existing Thales TH1507 140 GHz/1 MW gyrotron developed by KIT and SPC for W7-X [3,4], for which some components have been modified either to include state of the art design criteria or to optimize the operation at two different frequencies. This encompasses the use of a triode gun instead of a diode gun to keep control of the electron beam parameters at both frequencies, an increase of the cavity length to reach a reasonable normalized interaction length and quality factor at both frequencies, a hybrid-type launcher designed to provide a high output beam gaussian content for the two modes of operation, an adjustable last mirror to center the output beam at the window in case of necessity, an optimized collector cooling geometry and a diamond window

thickness corresponding to integer numbers of half-wavelengths at 84 and 126 GHz, thus maximizing the transmission at both frequencies. The first unit has been manufactured by Thales and delivered in the third quarter 2018 [5].

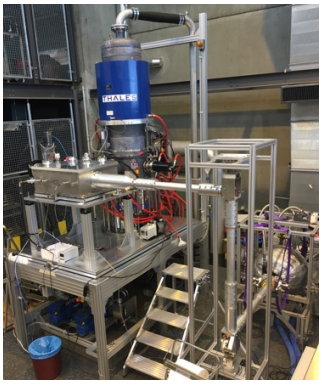

(a)

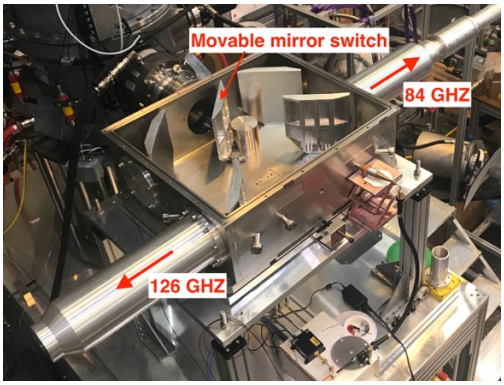

(b)

FIGURE 1. (a) The gyrotron tube during the commissioning phase, connected to the CNR load (on the bottom right). (b) The matching optic unit (MOU). When switching from 84 GHz to 126 GHz, the movable mirror is rotated by 90°.

LONG PULSE TEST RESULTS

After the initial short pulse testing period during which a ballistic load (<10 ms) was connected to the window, the matching optic unit (MOU) was put in place and the movable mirror was aligned to center the microwave beam at its exit. A section of 63.5 mm HE_{11} waveguide including 1 miter bend and one power monitor miter bend was used to transmit the power to the CNR load (see Fig. 1). The system was then closed, pumped, and the pulse extension phase could start using a standard procedure, and supported by monomode simulations (linear and non-linear). The results achieved so far are presented on Table 1. For the sake of simplicity, the same MOU-load configuration was used for the tests at 84 GHz and 126 GHz even though it is not optimal at the higher frequency. At 84 and 126 GHz, rf-powers very close or in excess of 1 MW were measured in the load, with pulse lengths larger than 1 s, with beam parameters close to the design ones. A key element of this successful result is that a triode gun is used, which gives the possibility to tune the electron beam pitch angle factor α to its optimal range (~1.3) for the magnetic fields corresponding to both frequencies, through an optimization of the anode voltage. No parasitic oscillation was detected in a 20 GHz bandwidth below the frequencies of the nominal modes.

TABLE 1. Long pulse (≥ 500 ms) performance of the gyrotron.

Parameter	X2	X3
Frequency [GHz]	84	126
Mode $TE_{m,p}$	$TE_{+17,5}$	$TE_{+26,7}$
Beam current Ib [A]	40	42
Cathode voltage V_k [kV] (RHVPS)	80	81.5
Beam energy V_b [kV] (2kV voltage depression)	78	79.5
Anode voltage [kV]	44	55.5
P_{rf} load [MW]	0.93	1.04
Load reflection [%] (est.)	4	4
TL losses (5 mirrors) [%] (est.)	0.8	0.8
Gyrotron int. mirrors losses (3) [%] (est.)	0.3	0.3
Launcher losses [kW] (meas.)	16	20
Cavity losses [kW] (meas.)	32	42
Stray radiation [kW] (est.)	60	40
Cavity RF-power [MW]	1.09 ± 5%	1.2 ± 5%
Electronic efficiency [%]	35 ± 1.5	36 ± 1.5
Frequency shift during pulse [MHz]	180	350

Accounting for the estimated, measured or calculated losses in the various sub-assemblies listed in Table 1, the cavity rf-power (i.e. the power lost by the electron beam) is estimated to be in excess of 1MW for both modes of operation. The frequency dependence of the cavity and launcher ohmic losses explains the higher losses at 126 GHz observed in Table 1, whereas the smaller wavelength and the fact that the launcher was preferentially optimized for 126 GHz explains the lower stray radiation at the higher frequency.

In the perspective of using the gyrotron on TCV, an interesting feature lies in the possibility to tune the output power in a very simple way: lowering the cathode voltage by 8-9 kV lead to a significant power decrease by 60 to 65%, while maintaining a stable oscillation on the design modes. This is illustrated in Figs. 2(a) and 2(d) (blue squares) at 84 GHz and 126 GHz respectively, together with the oscillation frequencies (once stabilized, red curves). Figures 2(b) and 2(e) show the time dependent oscillation frequency during a pulse. Consistently with the calculated cavity losses, the frequency shift observed at 126 GHz is larger than that at 84 GHz.

An excellent agreement was found between the experimental results and monomode simulations performed with the SPC code TWANG [6], shown on Figs 2(c) and 2(f), where power evaluated at the load is represented as a function of the anode voltage and the cathode voltage, and where a 2 kV beam depression has been taken into account. The smooth variation of the power with the cathode voltage, at constant anode voltage, is well reproduced, as well as the relative insensitivity to the anode voltage. Finally, the cathode voltage at which a mode jump occurs (79 kV and 82 kV respectively) corresponds almost exactly to the numerical prediction.

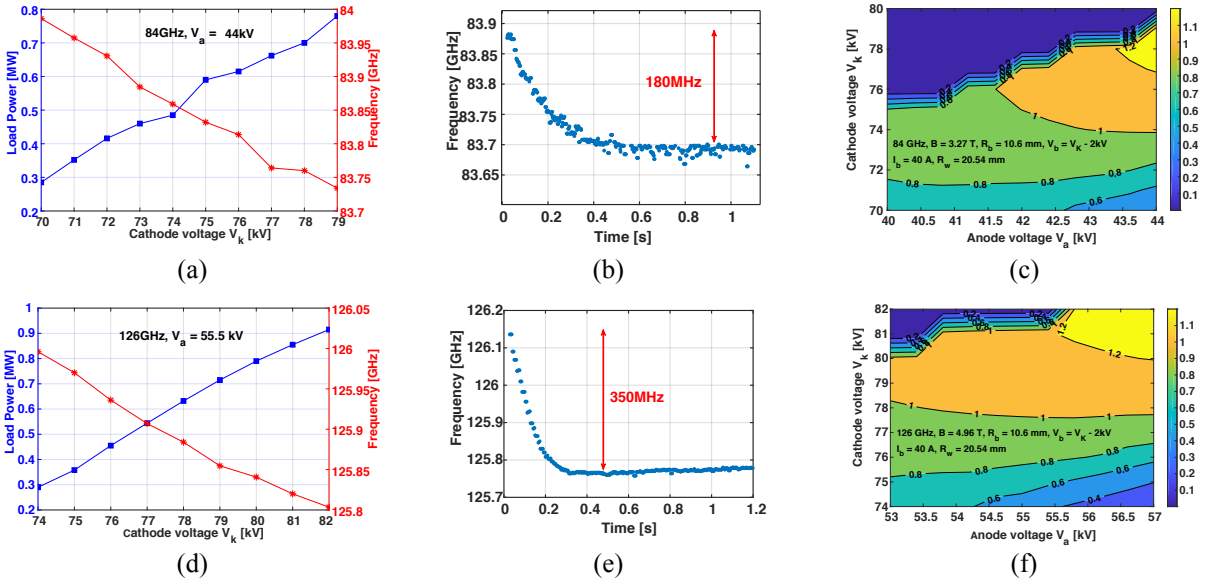

FIGURE 2. (a) and (d): Power measured in the load and oscillation frequency plotted against the cathode voltage at 84 GHz and 126 GHz respectively. (b) and (e): time dependence of oscillation frequency for a 0.93 MW pulse at 84GHz and a 0.992 MW at 126 GHZ. (c) and (f): Monomode simulations of the power in the load as a function of the anode voltage and cathode voltage.

Another evidence of the match between theory and experience was provided by a careful study of the oscillation start-up phase. The anode power supply risetime is relatively slow (ca. 20 ms), and spurious cavity modes can be excited during the ramp-up. A harmful (associated to a significant outgassing) counter-rotating mode $TE_{-23,8}$ at 125.75 GHz, present for a few ms only, was first detected. An optimization of the electron beam radius resulted in conditions in which the counter-rotating is no longer excited. However, it was replaced by the much less problematic co-rotating adjacent mode $TE_{+25,7}$ at 123.37 GHz. Taking the actual time-dependent anode voltage and estimating the corresponding pitch angle, α, the starting current of competing modes can be calculated. The top graph of Fig. 3 represents the actual electron beam current (black curve), as well as (among others) the starting current of the mode $TE_{+25,7}$ (yellow curve) and the one of the nominal mode $TE_{+26,7}$ (blue curve). In the time range 10-15 ms, the beam current is higher than the $TE_{+25,7}$ starting current, but lower than the $TE_{+26,7}$, whereas after 15 ms the second inequality is reversed. This means that the $TE_{+25,7}$ mode can be excited for times >10 ms and the $TE_{+26,7}$ mode for times >15 ms. This corresponds almost exactly to the experimental spectrogram shown on the bottom graph, where the $TE_{+25,7}$ mode is first observed, and then superseded by the $TE_{+26,7}$ through mode competition.

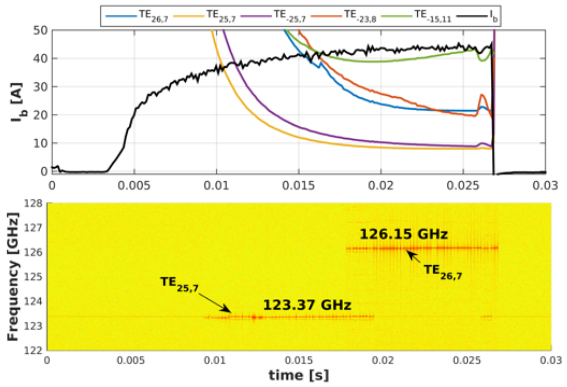

FIGURE 3. Top: Beam current during start-up phase and time-dependent starting currents of a few modes. Bottom: spectrogram during the same phase.

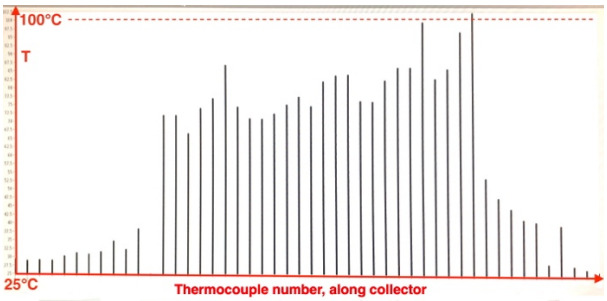

FIGURE 4. Longitudinal temperature profile on the non-depressed collector in presence of 7Hz modulation and 2Hz AM. The profile is more uniform than with 7Hz modulation only.

The robust and reproducible behavior of the tube constitutes a validation of the design changes. In addition, a modification of the longitudinal electron beam sweeping on the collector consisting in amplitude modulating the usual 7 Hz sweeping at 2 Hz allowed keeping the temperature profile quite flat, with a maximal temperature (122°C) well within the safe range, as illustrated on Fig. 4.

The pulse lengths achieved so far at the nominal power are of the order of 1 s. The limitations come from outgassing in the MOU due to stray radiation at 84 GHz, and from ripples in the anode voltage causing a mode loss at 126 GHz. The improvements necessary to better dissipate the stray rf-power deposited in the MOU and to stabilize the anode voltage are underway.

CONCLUSION AND OUTLOOK

The first prototype of dual-frequency gyrotron at 84 GHz and 126 GHz for TCV has been delivered by Thales and commissioned at SPC. The nominal power of 1 MW has been reached at both frequencies, with electronic efficiencies of the order of 35%, suggesting that an efficiency of 50% could be reached if a depressed collector was used. The design evolutions – increased cavity length, triode gun, hybrid-type launcher, improved collector cooling and sweeping scheme – have been validated. An excellent agreement was found between the experimental observations and numerical simulations performed with the monomode code TWANG. In addition, no parasitic oscillation has been detected. The extension to the nominal pulse length (2 s) will be carried out once present limitations (MOU at 84 GHz and anode power supply) have been overcome. The second tube will be delivered in June 2019 and the first operation on TCV is foreseen during the 2nd half of 2019.

ACKNOWLEDGMENTS

This work is partially supported by the Swiss National Science Foundation. This work has been carried out within the framework of the EUROfusion Consortium and has received funding from the Euratom research and training programme 2014-2018 and 2019-2020 under grant agreement No 633053. The views and opinions expressed herein do not necessarily reflect those of the European Commission.

REFERENCES

1. A. Fasoli et. al., Nucl. Fusion **55**(4), 043006 (2015).
2. S. Alberti et. al., EPJ Web of Conferences **157**, 03001 (2017).
3. S. Alberti et. al., Fusion Engineering and Design **53**, 387 (2001).
4. J. Jelonnek et. al.,IEEE Trans. on Plasma Science **42**(5), 1135 (2014).
5. R. Marchesin et. al., Proc. of IEEE IVEC 2019, Busan, South Korea.
6. J. Genoud et. al., Physics of Plasmas **23**(4), 043101 (2016).